

Chapter 7

Quantifying Human-Humanoid Imitation Activities

7.1 Human-Humanoid Imitation Experiment

previous chapter

We conducted an experiment in the context of human-humanoid imitation (HHI) activities where participants were asked to imitate repetitions of simple horizontal and vertical arm movements performed by NAO, a humanoid robot from Aldebaran Gouaillier et al. (2009). Such simple movements were repeated ten times for the participant as the robot performed those arm movements in a face-to-face imitation activity. Additionally, wearable inertial measurement unit (IMU) sensors were attached to the right hand of the participant and to the left hand of the robot (Figure 7.1 A,C). Data was then collected at a sampling rate of 50Hz with four NeMEMSi IMU sensors which provide tri-axial data of the accelerometer, gyroscope and magnetometer sensors and quaternions Comotti et al. (2014). A further description of the NeMEMSi IMU sensors is given in Appendix B.

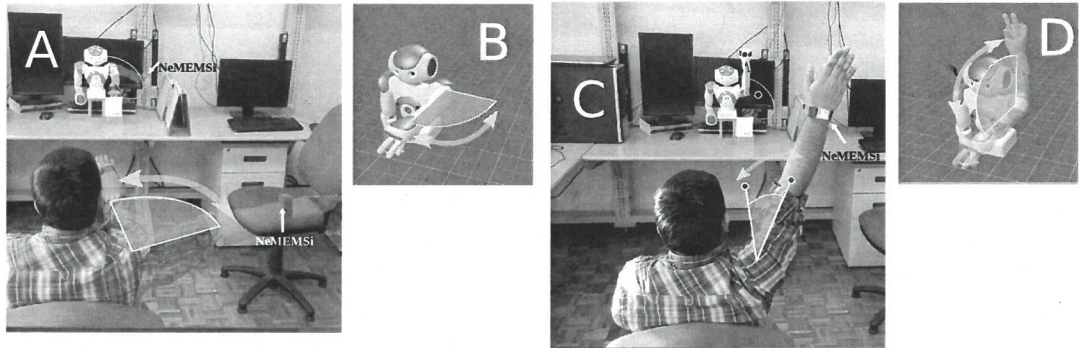


Fig. 7.1 Human-humanoid imitation activities. Face-to-face human-humanoid imitation (HHI) activities for (A) HHI of horizontal arm movement, (B) Humanoid horizontal arm movement, (C) HHI of vertical arm movement, and (D) Humanoid vertical arm movement.

7.1.1 Experiment of HHI activities

In the human-humanoid imitation (HHI) experiment four neMEMSi sensors Comotti et al. (2014) were used in which two sensors were attached to the right hand of the participant and two sensors were attached to the left hand of the humanoid robot. Then, each participant was asked to imitate repetitions of simple horizontal and vertical arm movements performed by the humanoid robot in the following conditions: (i) ten repetitions of horizontal arm movement at normal (HN) and faster (HF) speed (Figure 7.1 A), and (ii) ten repetitions of vertical arm movement at normal (VN) and faster (VF) speed (Figure 7.1 C). The normal and faster speed of arm movements is defined by the duration in number of samples of one repetition of NAO's arm movements. We select NAO's arm movements duration to distinguish between normal and faster arm movements as NAO's movements have less variation between repetition to repetition. The duration for one repetition of the horizontal arm movement at normal speed, HN, is about 5 seconds considering that each repetition last around 250 samples. For horizontal arm movement at faster speed, HF, each repetition were performed in around 2 seconds which correspond to 90 samples of data. The vertical

7.1 Human-Humanoid Imitation Experiment

arm movement at normal speed, VN, were performed in 6 seconds which is around 300 samples of data. For vertical arm movement at faster speed, VF, each repetition lasts about 2.4 seconds which correspond to 120 samples of data. To visualise the distinction between normal and faster speed for horizontal and vertical arm movements, Fig 7.2 shows smoothed time series for axes Z and Y of the gyroscope sensors with four window lengths: 2-sec (100-samples), 5-sec (250-samples), 10-sec (500-samples) and 15-sec (750-samples).

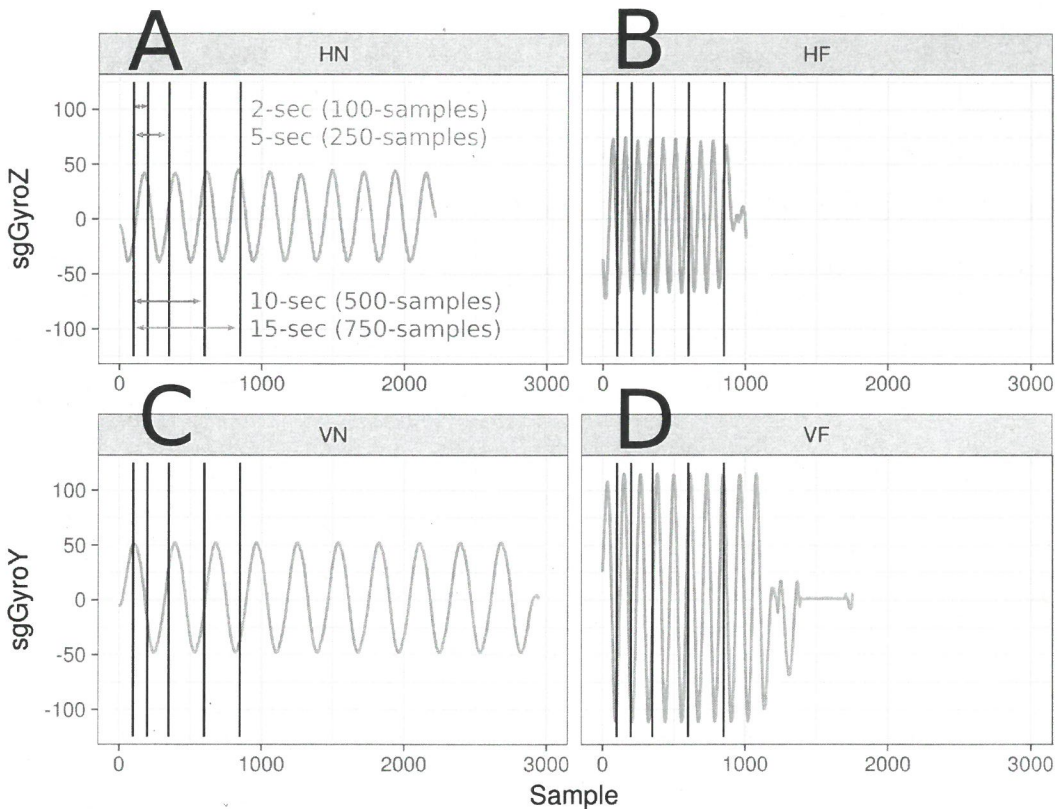


Fig. 7.2 Time series duration of horizontal and vertical arm movements. Time series of smoothed data from gyroscope sensor for different speed arm movements performed by NAO: (A) Horizontal Normal arm movement, HN, (B) Horizontal Faster arm movement, HF, (C) Vertical Normal arm movement, VN, and (D) Vertical Faster arm movement, VF. Additionally, (A) shows window sizes for 2-seconds (100 samples), 5-seconds (250 samples), 10-seconds (500 samples) and 15-seconds (750 samples) which are also presented in (B), (C) and (D). R code to reproduce figure is available Xochicale (2018).

7.1.2 Time-series from Inertial Measurement Units

Raw data

Considering the work of Shoaib et al. (2016) which provided evidence of an improvement in recognition activities when combining data from accelerometer and gyroscope, We ~~were~~ focus our analysis from data of the accelerometer and gyroscope of the NeMEMs sensors Comotti et al. (2014) and leave the data of the magnetometer and quaternions for further investigation because of their possible variations with regard to magnetic disturbances.

Data from the accelerometer is defined by triaxial time series $A_x(n)$, $A_y(n)$, $A_z(n)$ which forms the matrix \mathbf{A} (Eq. 7.1), and the same for data from the gyroscope which is defined by triaxial time-series of $G_x(n)$, $G_y(n)$, $G_z(n)$ representing the matrix \mathbf{G} (Eq. 7.2). Both triaxial time series of each sensor, a and g , are denoted with its respective axes subscripts x, y, z , where n is the sample index and N is the same maximum length of all axes for the time series. Matrices \mathbf{A} and \mathbf{G} are represented as follow

$$\mathbf{A} = \begin{pmatrix} A_x(n) \\ A_y(n) \\ A_z(n) \end{pmatrix} = \begin{pmatrix} a_x(1), a_x(2), \dots, a_x(N) \\ a_y(1), a_y(2), \dots, a_y(N) \\ a_z(1), a_z(2), \dots, a_z(N) \end{pmatrix}, \quad (7.1)$$

$$\mathbf{G} = \begin{pmatrix} G_x(n) \\ G_y(n) \\ G_z(n) \end{pmatrix} = \begin{pmatrix} g_x(1), g_x(2), \dots, g_x(N) \\ g_y(1), g_y(2), \dots, g_y(N) \\ g_z(1), g_z(2), \dots, g_z(N) \end{pmatrix}, \quad (7.2)$$

where n is the sample index and N is the same maximum length of all axes for the time series.

7.1.3 Postprocessing data

After the collection of raw data from four NeMEMsi sensors, time synchronisation alignment and interpolation were performed in order to create time series with the same length and synchronised time. We refer the reader to Appendix B for technical information about the time synchronisation process and IMU sensors.

Data normalization

Data is normalised to have zero mean and unit variance using sample mean and sample standard deviation Ioffe and Szegedy (2015). The sample mean and sample standard deviation using $x(n)$ is given by

$$\mu_{x(n)} = \frac{1}{N} \left(\sum_{i=1}^N x(i) \right), \quad \sigma_{x(n)} = \sqrt{\frac{\sum_{i=1}^N (x(i) - \mu_{x(n)})^2}{N-1}}, \quad (7.3)$$

then the normalised data, $\hat{x}(n)$, is computed as follows

$$\hat{x}(n) = \frac{x(n) - \mu_{x(n)}}{\sigma_{x(n)}}. \quad (7.4)$$

Smoothing data

Using a low-pass filter is the common way to either capture the low frequencies that represent %99 of the human body energy or to get the gravitational and body motion components of accelerations Anguita et al. (2013). However, for this work the main focus is on the conservation of the structure of the time series in terms of the width and heights where, for instance, Savitzky-Golay filter can help to accomplish such task Press et al. (1992). Savitzky-Golay filter is based on the principle of moving window average which preserves the area under the curve (the zeroth moment) and its mean position in time (the first moment) but the line width (the second moment) is violated

Quantifying Human-Humanoid Imitation Activities

and that results, for example, in the case of spectrometric data where a narrow spectral line is presented with reduced height and width. The aim of Savitzky-Golay filtering is to find the filter coefficients c_n that preserve higher momentums which are based on local least-square polynomial approximations Press et al. (1992); Savitzky and Golay (1964); Schafer (2011). Hence, Savitzky-Golay coefficients are therefore computed using an R function `sgolay(p,n,m)` where p is the filter order, n is the filter length (must be odd) and m is the m -th derivative of the filter coefficients signal R developers (2014). Smoothed signal is represented with a tilde over the original signal: $\tilde{x}(n)$.

Window size data

With regard to the window size, Shoaib et al. (2016) investigated its effects using seven window lengths (2, 5, 10, 15, 20, 25, 30 seconds) and combination of inertial sensors (accelerometer, gyroscope and linear acceleration sensor) in activity recognition performance for repetitive activities (walking, jogging and biking) and less repetitive activities (smoking, eating, giving a talk or drinking a coffee). Similarly, Shoaib et al. (2016) experimented with different window size effect to conclude that the increase of window size improved the recognition of complex activities because these required a large window to learn the repetitive motion patterns. Also, Shoaib et al. (2016) concluded that the use of large window size improve the recognition performance of less repetitive activities which mainly involve random hand gestures.

For the activities in this thesis which are mainly repetitive, we selected only four window sizes: 2-s window (100 samples), 5-s window (250 samples), 10-s (500 samples) and 15-s window (750 samples) (Figure 7.2).

start this chapter here

7.2 Human-Humanoid Imitation Activities

7.2 Human-Humanoid Imitation Activities

We investigated the robustness and weaknesses of the reconstructed state spaces (RRSs) using the uniform time-delay embedding technique (UTDE) and recurrence plots (RPs) for recurrent quantification analysis (RQA) methodologies in the following conditions:

- Three levels of smoothness for the normalised data (`sg0zmuv`, `sg1zmuv` and `sg2zmuv`), computed from two different filter lengths (29 and 159) with the same polynomial degree of 5 using the function `sgolay(p,n,m)` signal R developers (2014),
- Four velocities arm movement activities: horizontal normal (HN), horizontal faster (HF), vertical normal (VN), and vertical faster (VF), and
- Four window lengths: {2-sec (100 samples), 5-sec (250 samples), 10-sec (500 samples) and 15-sec (750 samples) }.

7.2.1 Time series

After the data collection in the experiment, raw time series were windowed, normalised and smoothed. We only present 10-sec (500 samples) window length time series, due to space limitations, for three participants (p01, p01 and p03) performing horizontal arm movements (axis GyroZ) and vertical arm movements (axis GyroY) (Figs 7.3 and 7.4). We consider different levels of smoothness of the normalised data with two different Savitzky-Golay filter lengths (29 and 159) with the same polynomial degree of 5 using `sgolay(p,n,m)` signal R developers (2014).

I don't think there are 'space' problems for a thesis - perhaps choose of 3 to make comparison easier⁵⁵. Other data in Appendix?

Quantifying Human-Humanoid Imitation Activities

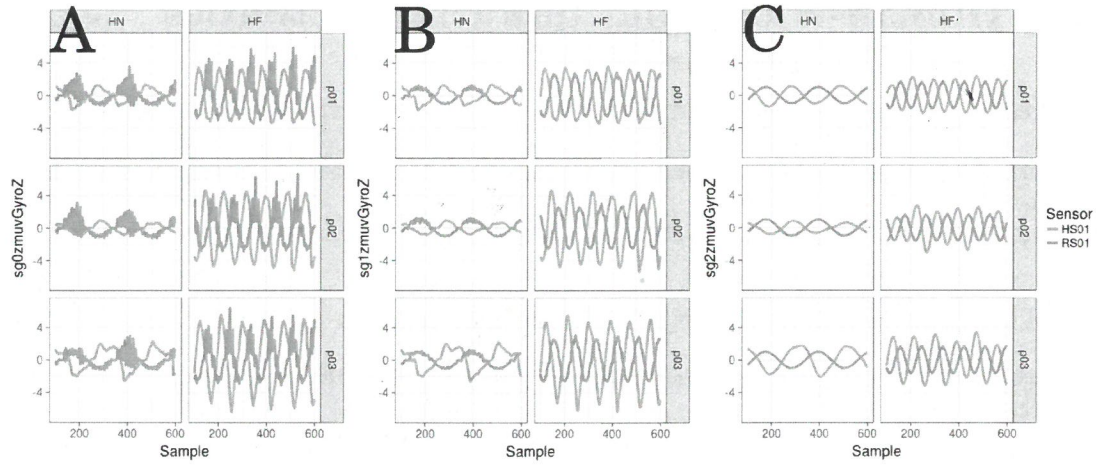


Fig. 7.3 Time series for horizontal arm movements. (A) raw-normalised ($sg0zmuvGyroZ$), (B) normalised-smoothed 1 ($sg1zmuvGyroZ$) and (C) normalised-smoothed 2 ($sg2zmuvGyroZ$). Time series are only for three participants (p01, p02, and p03) for horizontal movements in normal and faster velocity (HN, HF) with the normalised GyroZ axis ($zmuvGyroZ$) and with one sensor attached to the participant (HS01) and other sensor attached to the robot (RS01). R code to reproduce the figure is available from Xochicale (2018).

7.2.2 UTDE for time series in the context of human-robot interaction

The first step to create reconstructed state spaces is to compute the minimum embedding parameters which are computed in the following section.

Minimum Embedding Parameters

Considering the time series for twenty participants, minimum embedding dimensions were computed using False Nearest Neighbour for horizontal and vertical arm movements. Figs 7.5 and 7.6 show that minimum embedding values appear to be more constant for sensor RS01 than the slightly variations of such values for sensor HS01. It can also be seen that there is a minor decrease of minimum embedding values as smoothness of time series increase. To have an overall minimum dimension value that

7.2 Human-Humanoid Imitation Activities

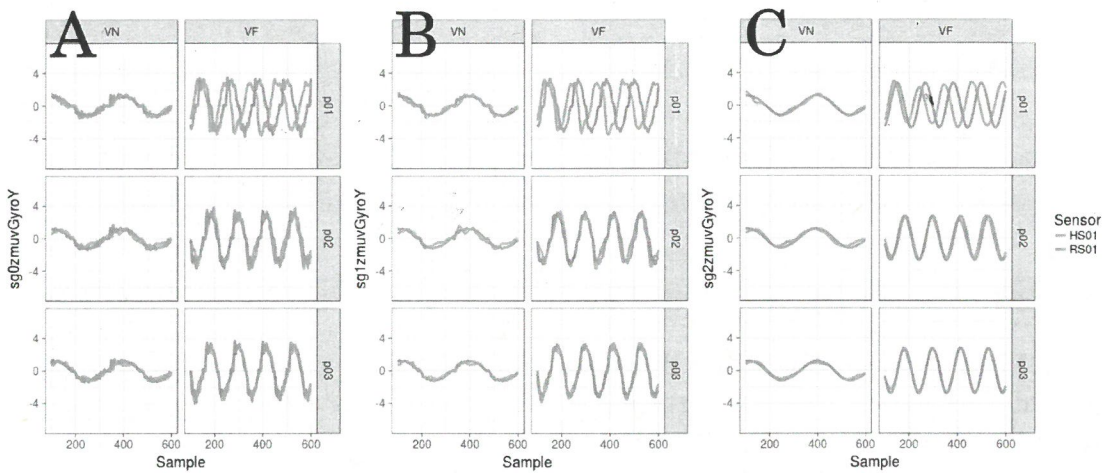


Fig. 7.4 Time series for vertical arm movements. (A) raw-normalised ($sg0zmuvGyroY$), (B) normalised-smoothed 1 ($sg1zmuvGyroY$) and (C) normalised-smoothed 2 ($sg2zmuvGyroY$). Time series are only for three participants (p01, p02, and p03) for vertical movements in normal and faster velocity (VN, VF) with the normalised GyroY axis ($zmuvGyroY$) and with one sensor attached to the participant (HS01) and other sensor attached to the robot (RS01). R code to reproduce the figure is available from Xochicale (2018).

represent participants, sensors and activities, a sample mean were computed over all the minimum values in Figs 7.5 and 7.6 which results in $\bar{m}_0 = 6$.

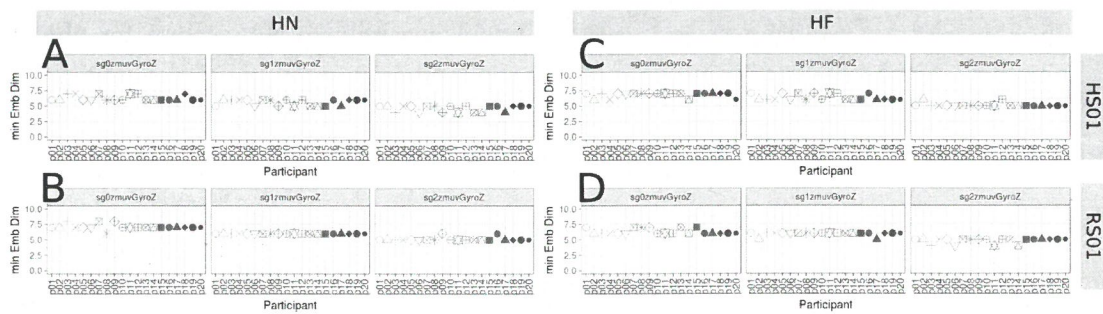


Fig. 7.5 Minimum embedding dimensions for horizontal arm movements. (A, B) Horizontal Normal (HN), (C, D) Horizontal Faster (HF) movements, (A, C) sensor attached to participants (HS01), and (B, D) sensor attached to robot (RS01). Minimum embedding dimensions are for twenty participants (p01 to p20) with three smoothed signals ($sg0zmuvGyroZ$, $sg1zmuvGyroZ$ and $sg2zmuvGyroZ$) and window lenght of 10-sec (500 samples). R code to reproduce the figure is available from Xochicale (2018).

idea to anticipate
this in your Metrics
chapter → or
you move your parts
on page 59/60 earlier

Quantifying Human-Humanoid Imitation Activities

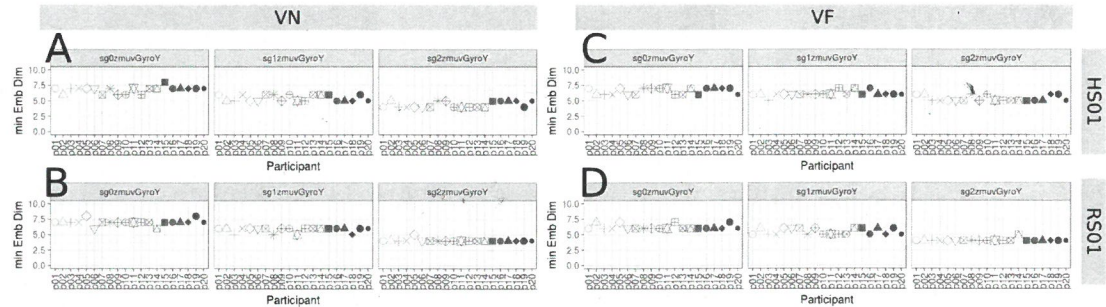


Fig. 7.6 Minimum embedding dimensions for vertical arm movements. (A, B) Vertical Normal (VN), (C, D) Vertical Faster (VF) movements, (A, C) sensor attached to participants (HS01), and (B, D) sensor attached to robot (RS01). Minimum embedding dimensions are for twenty participants (p01 to p20) with three smoothed signals ($sg0zmuvGyroY$, $sg1zmuvGyroY$ and $sg2zmuvGyroY$) and window length of 10-sec (500 samples). R code to reproduce the figure is available from Xochicale (2018).

Similarly, considering the time series for twenty participants, minimum delay values were computed as the first minimum values of the Average Mutual Information (AMI) for horizontal and vertical arm movements (Figs 7.7 and 7.8).

For horizontal arm movements, Fig 7.7A shows that values tend to be more spread as the smoothness is increased which is different for Fig 7.7C where values show no effect as the smoothness of time series increase. In contrast, Fig 7.7B shows the values are less spread as smoothness is increased which we believe the reason for that is due to the high frequencies on robots movements in the horizontal normal movement. However, values in Fig 7.7D tend to be spread as smoothness is increasing which are due to very different curves in the AMI. With regard to vertical arm movements, values in Figs 7.8A and 7.8C show an slightly increase of the spread values as the smoothness increase and values in Fig 7.8B appear to have less variation as the smoothness of the signals is increasing. However, that do not happen for the second smoothed values ($sg2zmuvGyroY$) in Fig 7.8D. We also computed an overall minimum delay value that represent participants, sensors and activities, using a sample mean of all values in Figs 7.7 and 7.8 which results in $\bar{\tau}_0 = 8$.

7.2 Human-Humanoid Imitation Activities

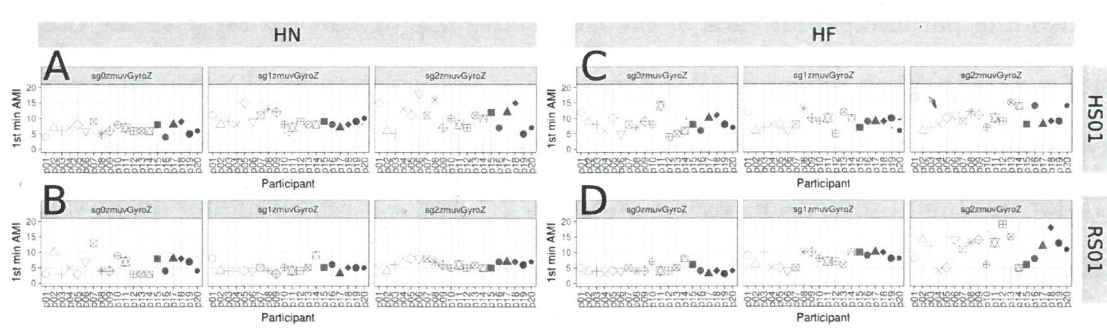


Fig. 7.7 First minimum AMI values for horizontal arm movements. (A, B) Horizontal Normal (HN), (C, D) Horizontal Faster (HF) movements, (A, C) sensor attached to participants (HS01), and (B, D) sensor attached to robot (RS01). First minimum AMI values are for twenty participants (p01 to p20) with three smoothed signals ($sg0zmuvGyroZ$, $sg1zmuvGyroZ$ and $sg2zmuvGyroZ$) and window lenght of 10-sec (500 samples). R code to reproduce the figure is available from Xochicale (2018).

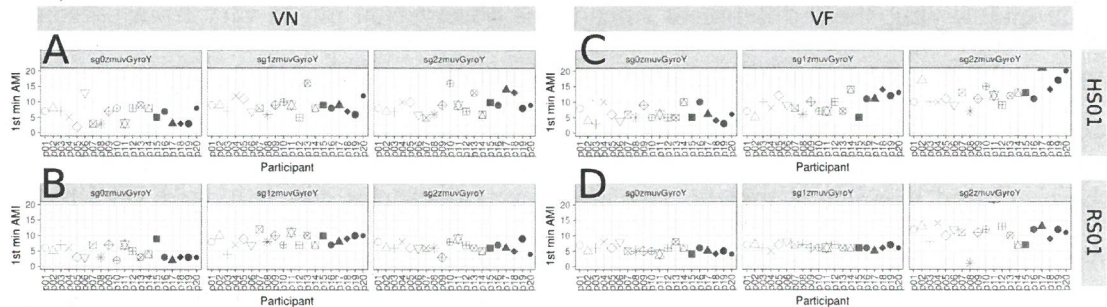


Fig. 7.8 First minimum AMI values for vertical arm movements. (A, B) Vertical Normal (VN), (C, D) Vertical Faster (VF) movements, (A, C) sensor attached to participants (HS01), and (B, D) sensor attached to robot (RS01). First minimum AMI values are for twenty participants (p01 to p20) with three smoothed signals ($sg0zmuvGyroY$, $sg1zmuvGyroY$ and $sg2zmuvGyroY$) and window lenght of 10-sec (500 samples). R code to reproduce the figure is available from Xochicale (2018).

Reconstructed state spaces Using UTDE

Although the implementation of Uniform Time-Delay Embedding for the reconstructed state space, one of the main challenges of the latter is the selection of embedding parameters because each time series is unique in terms of its structure (modulation of amplitude, frequency and phase) Bradley and Kantz (2015); Frank et al. (2010); Samà et al. (2013). With that in mind, the problem is not to compute individual

Quantifying Human-Humanoid Imitation Activities

embedding parameters for each of the time series but to deal with selecting of two parameters that can represent all the time series. Our solution for that was to compute a sample mean over all values in each of the conditions of the time series of Figs 7.5, 7.6 for minimum dimension values and Figs 7.7 and 7.8 for minimum delay values, resulting in an average minimum embedding parameters of ($\bar{m}_0 = 6$, $\bar{\tau}_0 = 8$). Then, the reconstructed state spaces were computed with ($\bar{m}_0 = 6$, $\bar{\tau}_0 = 8$) and the first three axis of the rotated data of the PCA are shown in Figs 7.9 for horizontal arm movements and Figs 7.10 for vertical arm movements.

~~One can~~
Evidently, it is easy to observe by eye the differences in each of the trajectories in the reconstructed state spaces (Figs 7.9, 7.10), however one might be not objective when quantifying those differences since those observation might vary from person to person. With that in mind, we tried to objectively quantify those differences using euclidean distances between the origin to each of the points in the trajectories, however these created suspicious metric, specially for trajectories which looked very messy. With that in mind, we computed Recurrence Quantification Analysis to objectively quantify the differences in each of the cases of the time series.

7.2.3 RPs and RQA for time series in the context of human-robot interaction

Recurrences Plots

Considering the time series of Figs 7.3 and 7.4, we computed its Recurrence Plots for horizontal arm movements (Fig 7.11) and for vertical arm movements (Fig 7.12) using the average embedding parameters ($m = 6$, $\tau = 8$) and an recurrence threshold of $\epsilon = 1$. With regard to the selection of recurrence threshold, Marwan et al. Marwan (2011) pointed out that choosing an appropriate recurrence threshold is crucial to get meaningful representations in RPs, however, for our work where quantifying movement

You
should
point
some
examples
out to
the
reader
What
are
figures
7.9 and 7.10
Showing?
What are
the relevant
or important
things to
notice?
I think
there
is at
least
another
page of
explanation to
provide here.

7.2 Human-Humanoid Imitation Activities

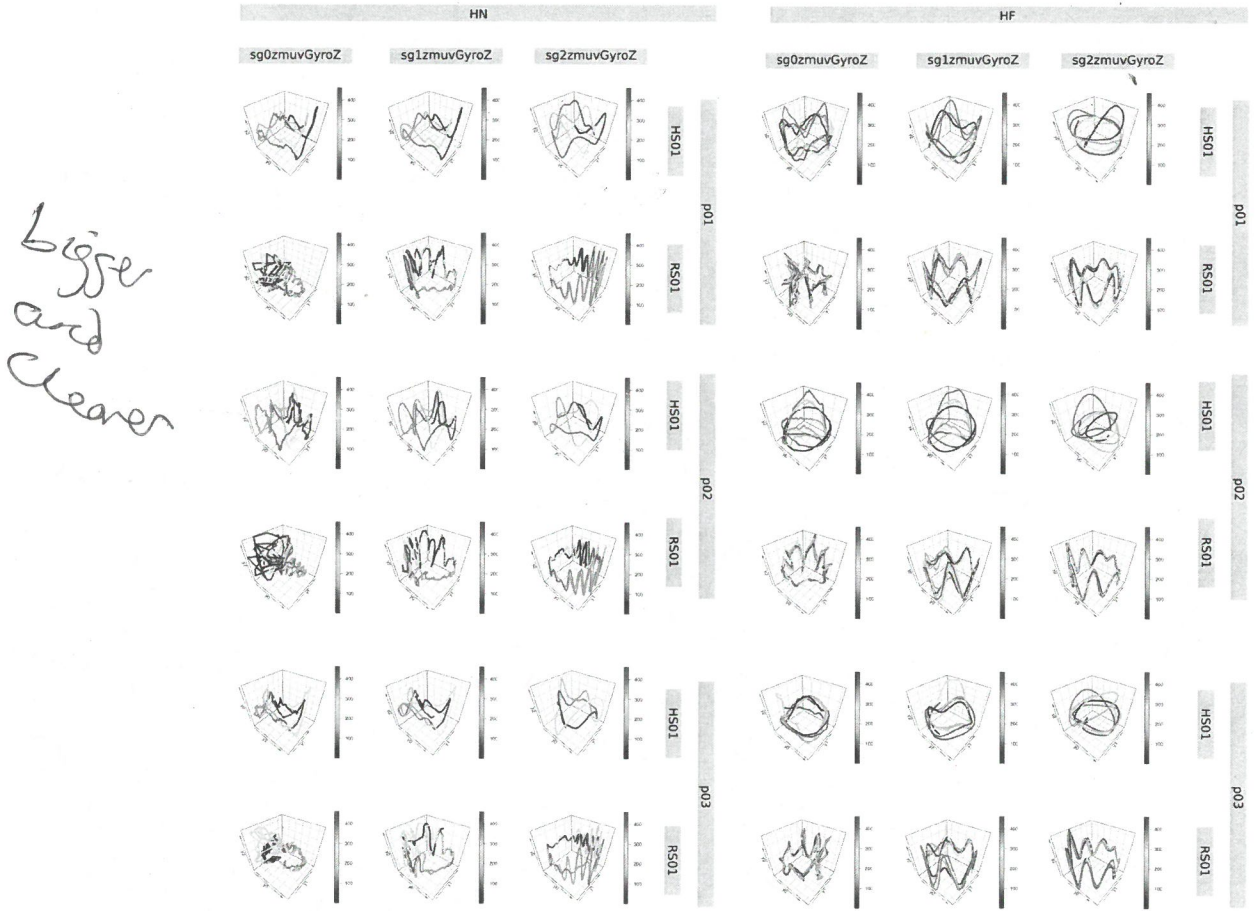


Fig. 7.9 RSSs for horizontal arm movements. Reconstructed state spaces for time series of Figure 7.3. Reconstructed state spaces were computed with embedding parameters $m = 6$, $\tau = 8$. R code to reproduce the figure is available from Xochicale (2018).

variability is our aim, we give little importance to the selection of the recurrence threshold as long as it is able to represent the dynamical transitions in each of the time series.

As similar as with the Reconstructed State Spaces, the differences in the RPs can be easily noticed by eye for different conditions of the time series (Figs 7.12, Fig 7.11), which lead us to apply Recurrence Quantification Analysis to have an objective quantification of each of the time series.

Quantifying Human-Humanoid Imitation Activities

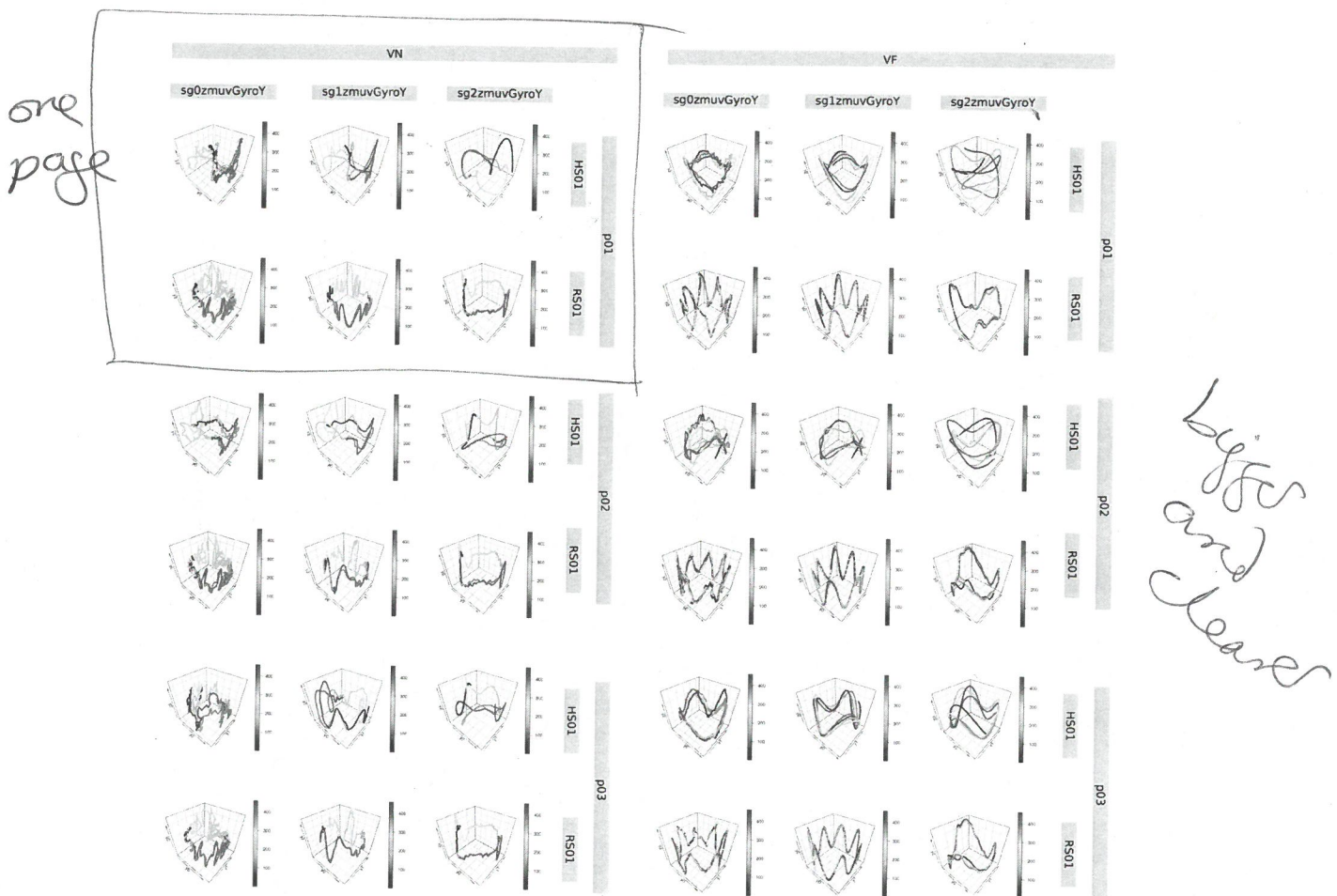


Fig. 7.10 RSSs for vertical arm movements. Reconstructed state spaces for time series of Figure 7.4. Reconstructed state spaces were computed with embedding parameters $m = 6$, $\tau = 8$. R code to reproduce the figure is available from Xochicale (2018).

Recurrence Quantification Analysis

RPs provided pattern formations for each of the time series conditions (Figs 7.11 and 7.12). Hence, the following four metrics of RQA metrics (REC, DET, RATIO and ENTR) are computed:

again-explain these figures and point at the important/relevant features. Don't assume the reader will⁶² see everything that you do.

7.2 Human-Humanoid Imitation Activities

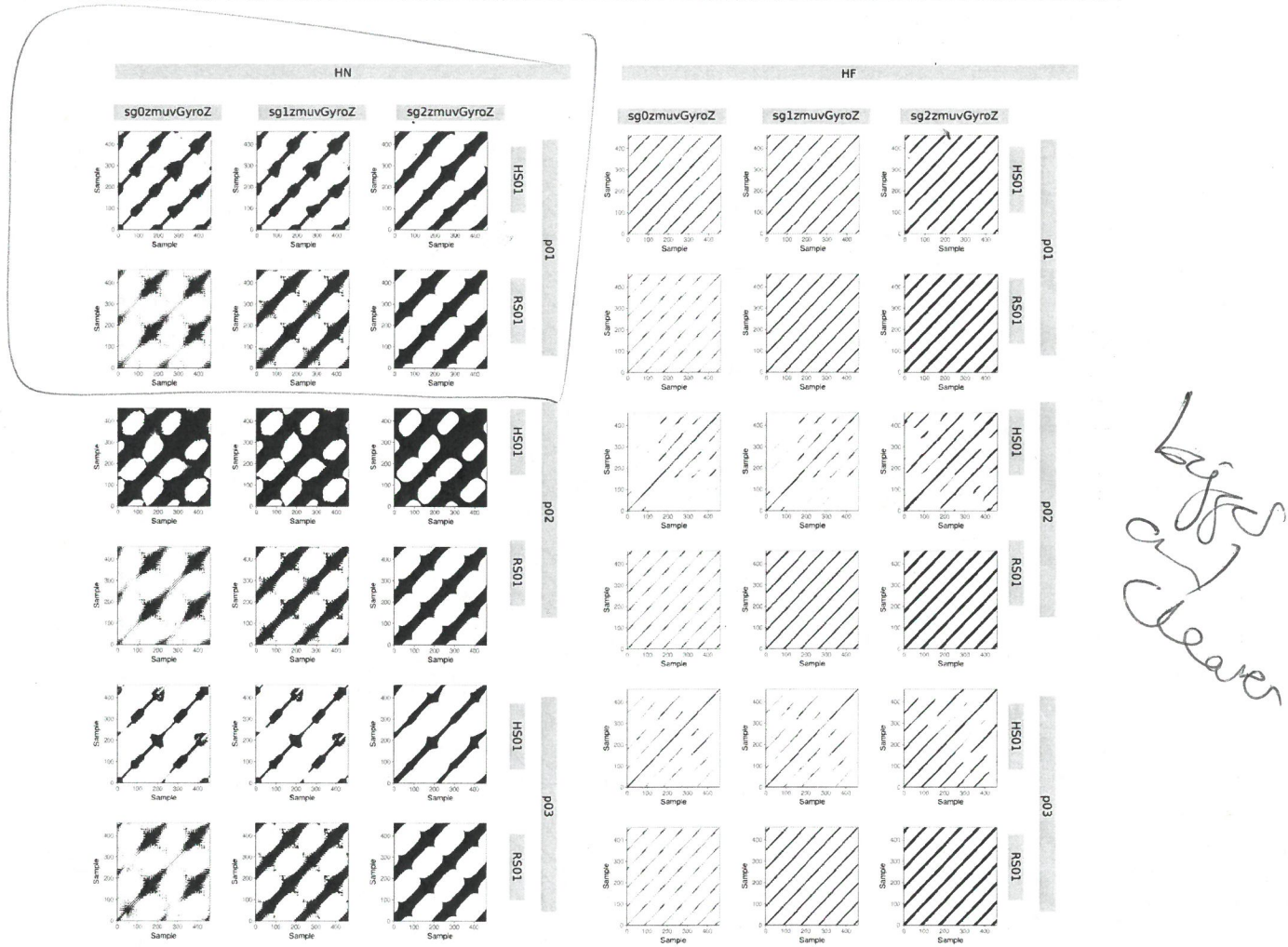


Fig. 7.11 RPs for horizontal arm movements. Recurrence plots were computed with embedding parameters $m = 6$, $\tau = 8$ and $\epsilon = 1$. R code to reproduce the figure is available from Xochicale (2018).

REC values

In Figs 7.13 and 7.14 can be seen that REC values are more spread for HN than HF movements with data coming from HS01 sensor. In contrast, REC values appear to be constant and present little variation for both HN and HF movements with data from the sensor attached to the humanoid robot RS01. With regard to the increase of smoothness of data (sg0zmuvGyroZ, sg1zmuvGyroZ and sg2zmuvGyroZ), REC values

Is this from one person? Explain what HS01 means and why use these data

Quantifying Human-Humanoid Imitation Activities



Fig. 7.12 RPs for vertical arm movements. Recurrence plots were computed with embedding parameters $m = 6$, $\tau = 8$ and $\epsilon = 1$. R code to reproduce the figure is available from Xochicale (2018).

present little variation as the smoothness is increasing for data from HS01 and REC values more similar as the smoothness is increasing for data from RS01.

DET values

~~Little can be said with regard to the variation of DET values as these change very little even for type of movement or type of sensor (Figs 7.15 and 7.16). With regard to the~~

7.2 Human-Humanoid Imitation Activities

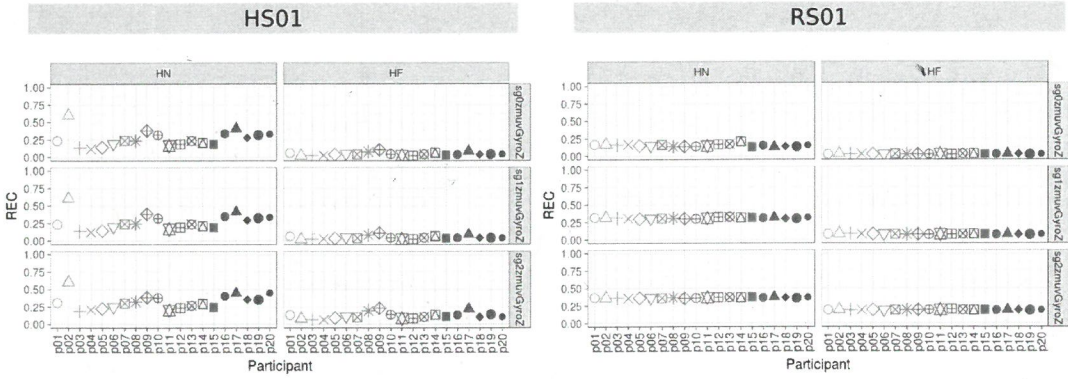


Fig. 7.13 **REC values for horizontal arm movements.** REC values (representing % of black dots in the RPs) for 20 participants performing HN and HF movements with sensors HS01, RS01 and three smoothed-normalised axis of GyroZ (sg0zmuvGyroZ, sg1zmuvGyroZ and sg2zmuvGyroZ). REC values were computed with embedding parameters $m = 6$, $\tau = 8$ and $\epsilon = 1$. R code to reproduce the figure is available from Xochicale (2018).

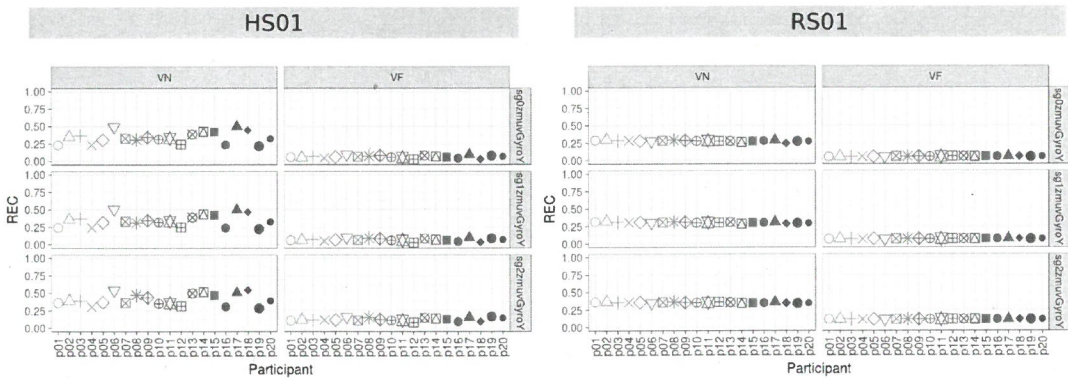


Fig. 7.14 **REC values for vertical arm movements.** REC values (representing % of black dots in the RPs) for 20 participants performing VN and VF movements with sensors HS01, RS01 and three smoothed-normalised axis of GyroY (sg0zmuvGyroY, sg1zmuvGyroY and sg2zmuvGyroY). REC values were computed with embedding parameters $m = 6$, $\tau = 8$ and $\epsilon = 1$. R code to reproduce the figure is available from Xochicale (2018).

smoothness of time series, DET values appear to be more similar as the smoothness of the data is increasing. *Would you expect them to change?*

Quantifying Human-Humanoid Imitation Activities

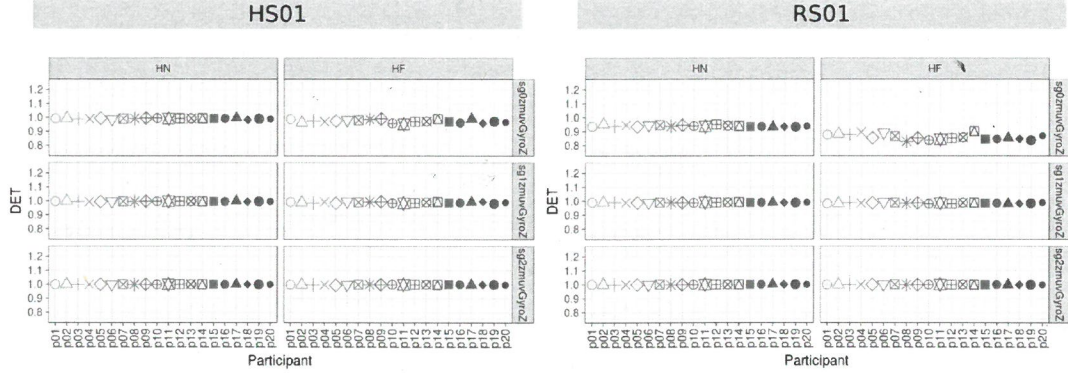


Fig. 7.15 **DET values for horizontal arm movements.** DET values (representing predictability and organisation of the RPs) for 20 participants performing HN and HF movements with sensors HS01, RS01 and three smoothed-normalised axis of GyroZ (sg0zmuvGyroZ, sg1zmuvGyroZ and sg2zmuvGyroZ). DET values were computed with embedding parameters $m = 6$, $\tau = 8$ and $\epsilon = 1$. R code to reproduce the figure is available from Xochicale (2018).

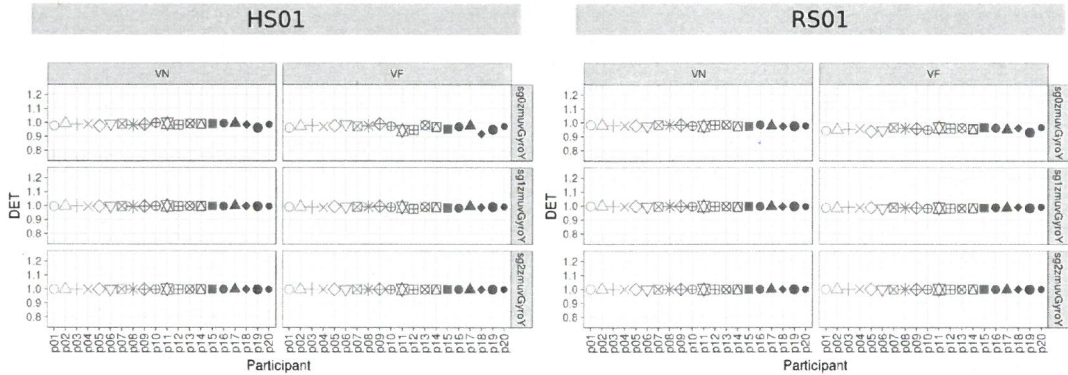


Fig. 7.16 **DET values for vertical arm movements.** DET values (representing predictability and organisation of the RPs) for 20 participants performing VN and VF movements with sensors HS01, RS01 and three smoothed-normalised axis of GyroY (sg0zmuvGyroY, sg1zmuvGyroY and sg2zmuvGyroY). DET values were computed with embedding parameters $m = 6$, $\tau = 8$ and $\epsilon = 1$. R code to reproduce the figure is available from Xochicale (2018).

RATIO values

RATIO values for HN movements vary less than HF movements for HS01 sensor which is similar behaviour of RATIO values for RS01 sensors in both vertical and horizontal

7.2 Human-Humanoid Imitation Activities

movements (Figs 7.17 and 7.18). It can also noticed a decrease of variation in RATIO values as the smoothness of the signal is increasing.

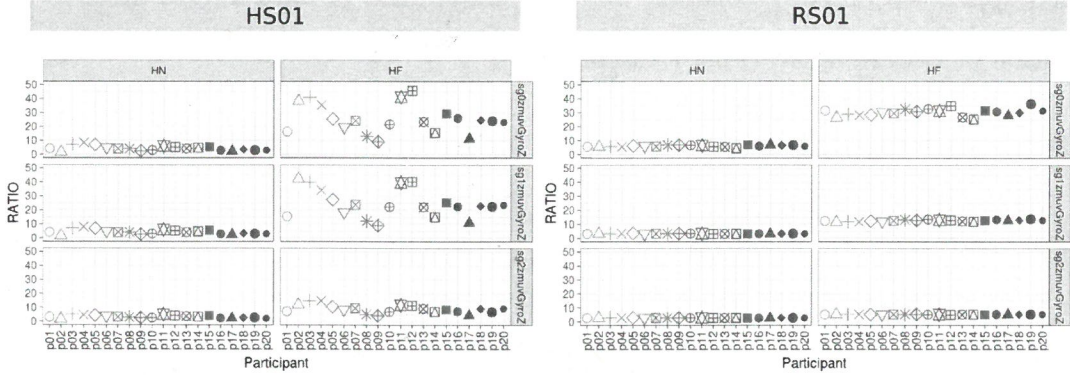


Fig. 7.17 RATIO values for horizontal arm movements. RATIO (representing dynamic transitions) for 20 participants performing HN and HF movements with sensors HS01, RS01 and three smoothed-normalised axis of GyroZ (sg0zmuvGyroZ, sg1zmuvGyroZ and sg2zmuvGyroZ). RATIO values were computed with embedding parameters $m = 6$, $\tau = 8$ and $\epsilon = 1$. R code to reproduce the figure is available from Xochicale (2018).

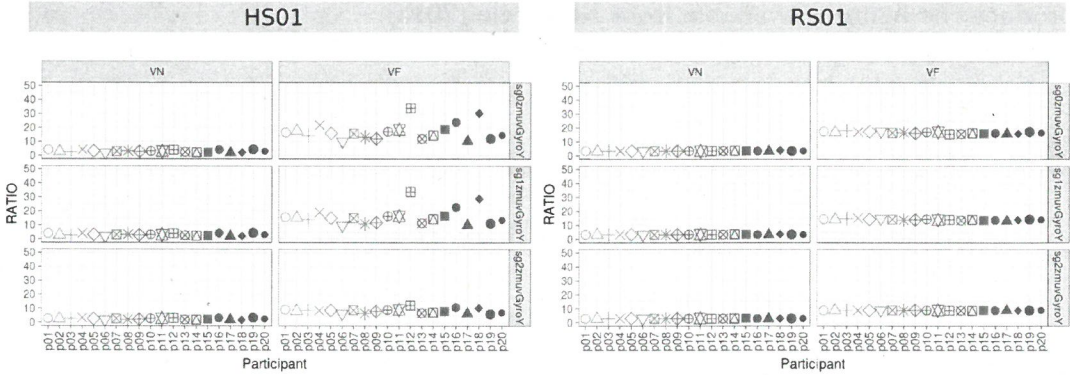


Fig. 7.18 RATIO values for vertical arm movements. RATIO (representing dynamic transitions) for 20 participants performing VN and VF movements with sensors HS01, RS01 and three smoothed-normalised axis of GyroY (sg0zmuvGyroY, sg1zmuvGyroY and sg2zmuvGyroY). RATIO values were computed with embedding parameters $m = 6$, $\tau = 8$ and $\epsilon = 1$. R code to reproduce the figure is available from Xochicale (2018).

Quantifying Human-Humanoid Imitation Activities

ENTR values

ENTR values show more variation for HS01 sensor than ENTR values for RS01 sensor which appear to be more constant and the smoothness of data affects little to the variation of ENTR values (Figs 7.19 and 7.20).

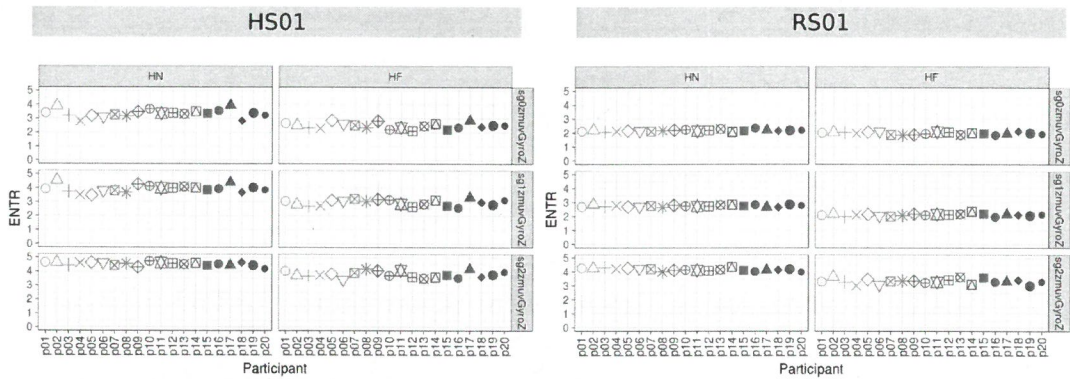


Fig. 7.19 ENTR values for horizontal arm movements. ENTR values (representing the complexity of the deterministic structure in time series) for 20 participants performing HN and HF movements with sensors HS01, RS01 and three smoothed-normalised axis of GyroZ ($sg0zmuvGyroZ$, $sg1zmuvGyroZ$ and $sg2zmuvGyroZ$). ENTR values were computed with embedding parameters $m = 6$, $\tau = 8$ and $\epsilon = 1$. R code to reproduce the figure is available from Xochicale (2018).

7.2.4 RQA metrics with different embedding parameters, recurrence thresholds, window lengths, levels of smoothness, and time series structures.

Zbilut et al. Zbilut and Webber (1992) established RQA metrics with the aim of determining embedding parameters, their method consisted on creating 3D surfaces with RQA metrics with an increase of embedding parameters (m and τ), then Zbilut et al. Zbilut and Webber (1992) explored fluctuations and gradual changes in the 3D surfaces that provide information about the embeddings. Much recently, Marwan et al. Marwan and Webber (2015) created 3D surfaces for visual selection of not only

This
Belongs
earlier
in the
Metrics
review
Chapt

7.2 Human-Humanoid Imitation Activities

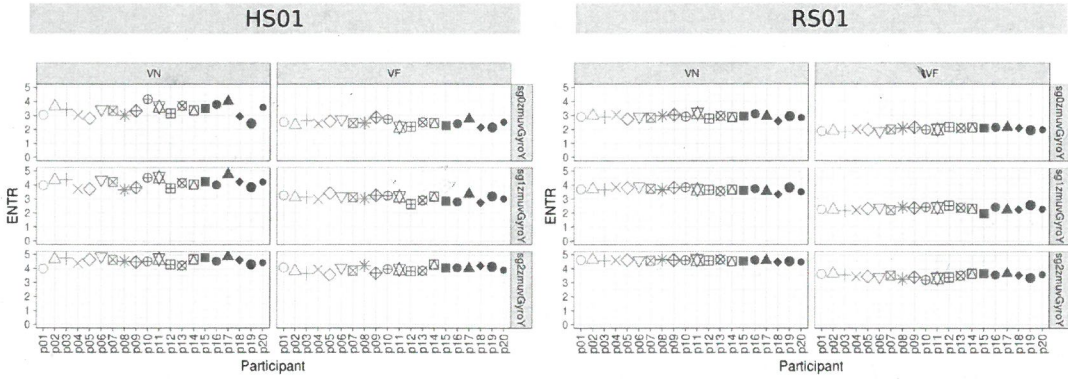


Fig. 7.20 ENTR values for vertical arm movements. ENTR values (representing the complexity of the deterministic structure in time series) for 20 participants performing VN and VF movements with sensors HS01, RS01 and three smoothed-normalised axis of GyroY (sg0zmuvGyroY, sg1zmuvGyroY and sg2zmuvGyroY). ENTR values were computed with embedding parameters $m = 6$, $\tau = 8$ and $\epsilon = 1$. R code to reproduce the figure is available from Xochicale (2018).

embedding parameters but also recurrence thresholds.) Following same methodologies, *explained* in chapter X, we explored the stability and robustness of RQA metrics (REC, DET, RATIO and ENTR) using 3D surfaces by an unitary increase of the pair embedding parameters ($0 \leq m \leq 10$, $0 \geq \tau \leq 10$) and a decimal increase of 0.1 for recurrence thresholds ($0.2 \geq \epsilon \leq 3$) (Fig. 7.21). We also computed 3D surfaces of RQA metrics for different sensors and different activities (Fig. 7.22). RQA metrics are also affected by the window length where for example four window lengths of 100, 250, 500 and 750 samples (Fig. 7.23). Three level of smoothness were computed for RQA metrics showing smoothed 3D surfaces ad the level of smoothness increase (Fig. 7.24). Similarly, 3D surfaces of RQA metrics were also computed for three participants (Fig. 7.25).

Quantifying Human-Humanoid Imitation Activities

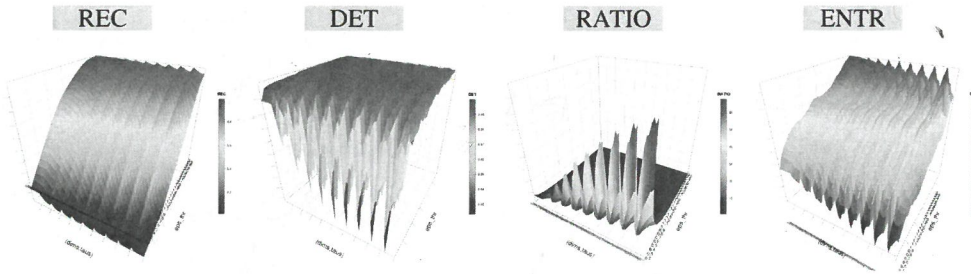


Fig. 7.21 **3D surfaces for RQA metrics.** 3D surfaces for REC, DET, RATIO and ENTR values with increasing pair embedding parameters ($0 \leq m \leq 10$, $0 \leq \tau \leq 10$) and recurrence thresholds ($0.2 \geq \epsilon \leq 3$). RQA metrics values for time series of participant p01 using HS01 sensor, HN activity and sg0zmuvGyroZ axis and 500 samples window length. R code to reproduce the figure is available from Xochicale (2018).

→ Every figure should have at least a paragraph out key features

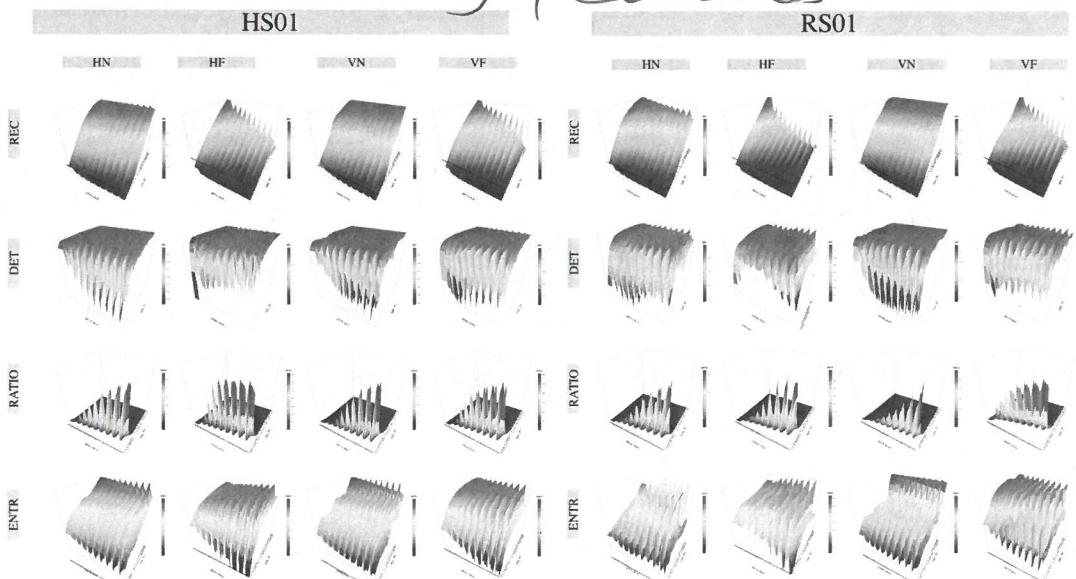


Fig. 7.22 **3D surfaces of RQA metrics for sensors and activities.** 3D surfaces with increasing embedding parameters and recurrence thresholds are for HS01 and RS01 sensors of HN, HF, VN and VF activities. RQA metrics values are for time series of participant p01 for sensors (HS01 and RS01), activities (HN, HF, VN and VF) and for sg0zmuvGyroZ axis with 500 samples window length. R code to reproduce the figure is available from Xochicale (2018).

Quantifying Human-Humanoid Imitation Activities

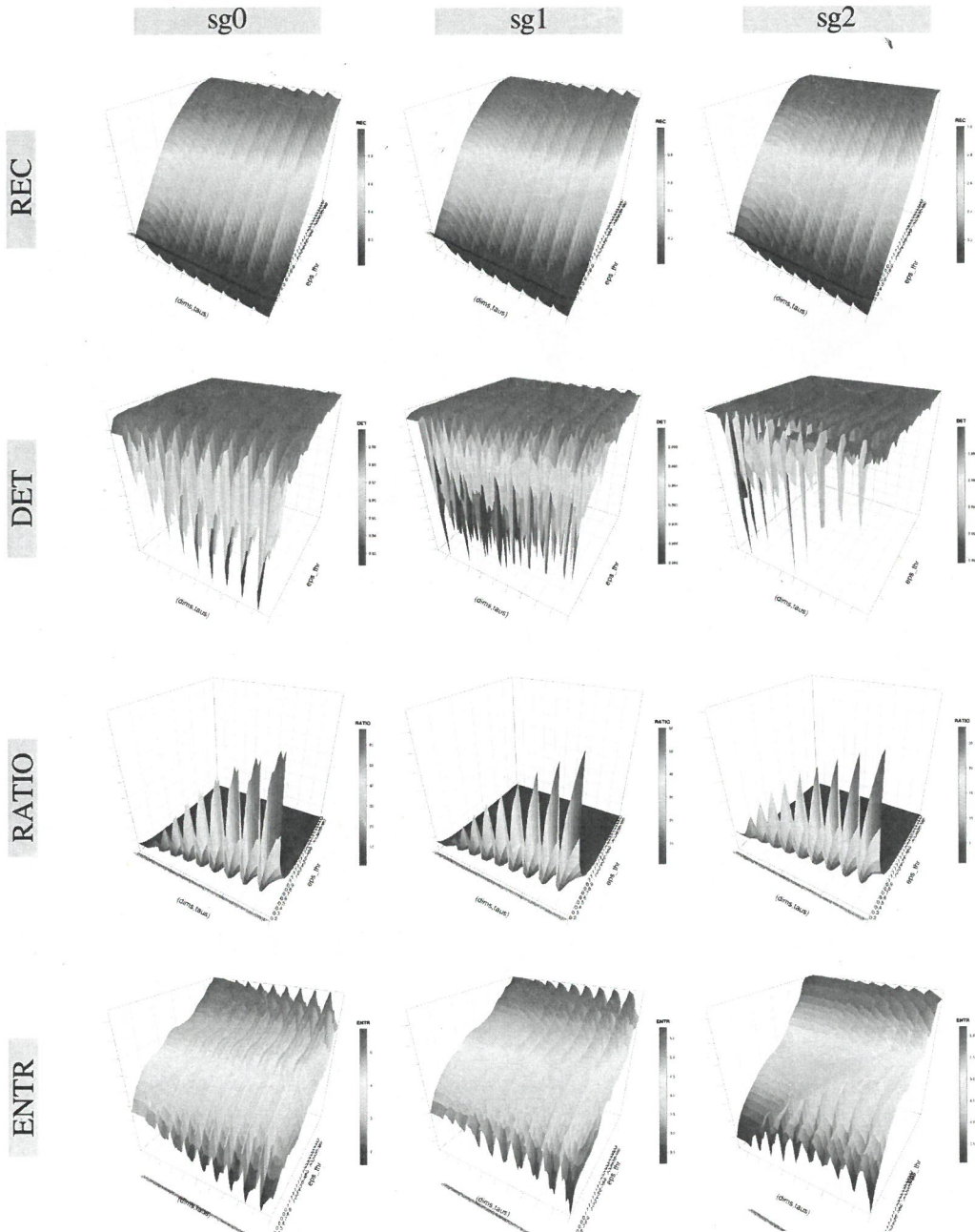


Fig. 7.24 3D surfaces for RQA metrics with three levels of smoothness. 3D surfaces of RQAs metric values with increasing embedding parameters and recurrence thresholds are for three levels of smoothness ($sg0_{zmuvGyroZ}$, $sg1_{zmuvGyroZ}$ and $sg1_{zmuvGyroZ}$). RQA metrics values are for time series of participant p01 using HS01 sensor, HN activity and 500 samples window length. R code to reproduce the figure is available from Xochicale (2018).

7.2 Human-Humanoid Imitation Activities

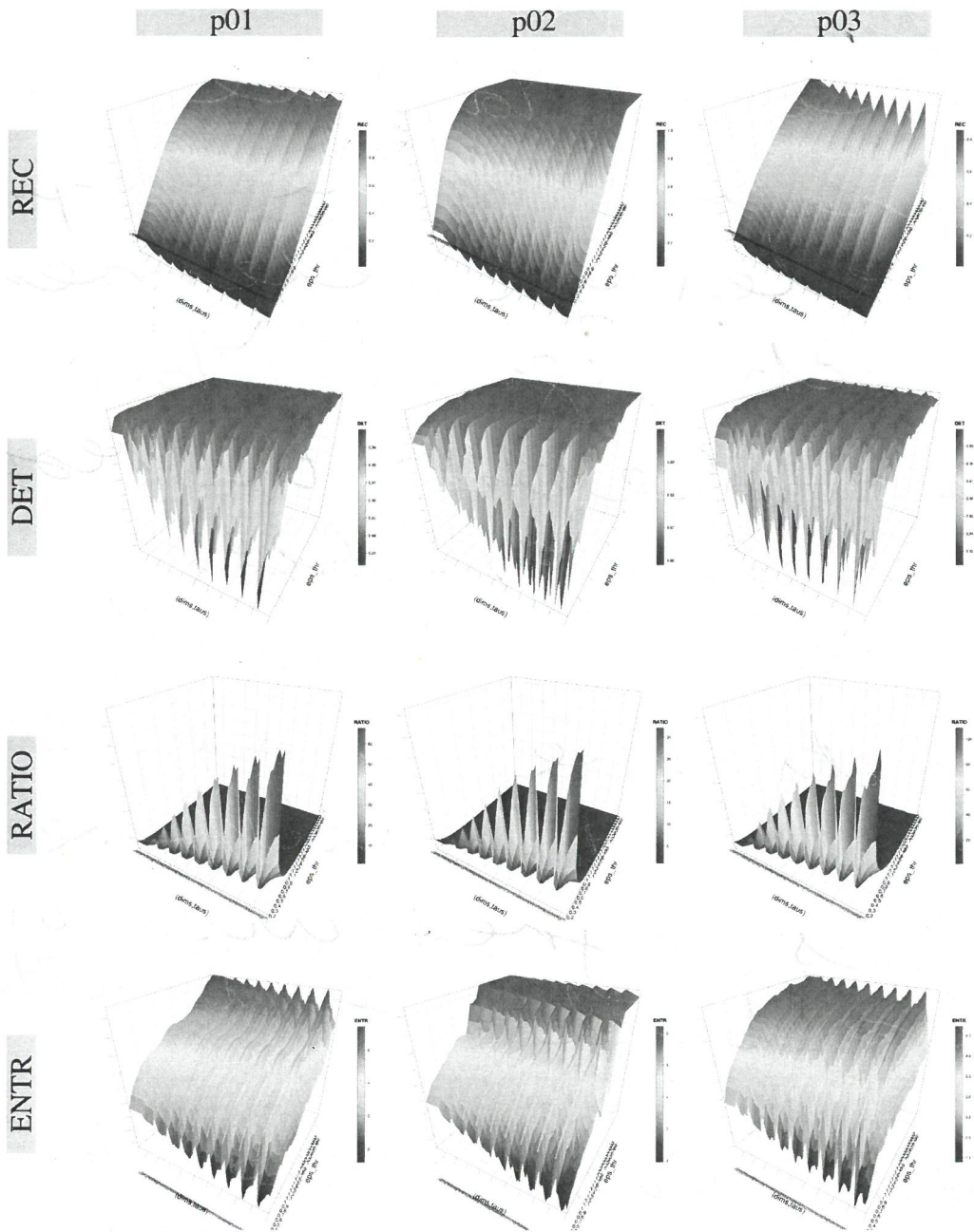


Fig. 7.25 3D surfaces for RQA metrics with three participants. 3D surfaces of RQAs metric values for participants p01, p02 and p03 with increasing embedding parameters and recurrence thresholds. RQA metrics values are for time series of HS01 sensor, HN activity and 500 samples window length. R code to reproduce the figure is available from Xochicale (2018).

I can see you have produced results but it is not obvious how these are meant to be interpreted. You need more explanation of the important and relevant elements of each figure. You need to say whether the results indicate variability. You need to say whether the results are as expected and whether different metrics agree with or contradict each other.

I am also worried that not including any of your other data means you risk the thesis looking like a single study Msc by Research rather than a PhD.